GEOMICROBIOLOGY JOURNAL
2021, VOL. 38, NO. 9, 809–815
https://doi.org/10.1080/01490451.2021.1954730

Taylor & Francis
Taylor & Francis Group

Biomineralization of Fe^{3+} to Nanosized γFe_2O_3 by *Haloferax alexandrinus* GUSF-1

Sanika Naik-Samant[a,b] and Irene J. Furtado[a]

[a]Department of Microbiology, Goa University, Taleigao Plateau, Goa, India; [b]Department of Biotechnology, Goa University, Taleigao Plateau, Goa, India

ABSTRACT

Hypersaline environment is a habitat with extreme osmotic conditions along with low A_w, serving as a home to extremely halophilic and halotolerant bacteria. The hypersaline environments, such as solar salterns located along the rivers, are exposed to fluxes of iron from iron ore transportation and other industrial wastes. The solar salterns often serve as a sink for metal intoxicants. Studies on archaea interaction with metal ions indicate the formation of minerals such as goethite, hematite, rhodochrosite, etc. However, studies exploring haloarchaeal candidates interacting with metals such as Fe^{3+} in a hypersaline growth condition are scarce. This study unveils for the first time formation of γFe_2O_3 from Fe^{3+} by the haloarchaeon, *Haloferax* sp. GUSF-1 thus implying the significance of the culture synthesizing minerals in hypersaline sediments. γFe_2O_3 is formed from Fe^{3+} by the haloarchaeon *Haloferax* sp. GUSF-1 (GenBank accession no.GU-1KF796625), under microaerophilic growth on sodium acetate. A 50 mg L^{-1} of Fe^{2+} and 30.6 mg L^{-1} of Fe^{3+} was detected inside the cells. Simultaneously, a brown-colored crystalline material deposited in the culture broth through an iron reductase inhibited by Zn^{2+} ions. The XRD of the deposit exhibited *d* values of 2.96, 2.514, 2.086, 1.6, and 1.45, while SEM-EDX displayed cubic and irregularly shaped minute particles with peaks for Fe at 0.6, 6.4, and 6.6 keV, respectively. TEM profiles revealed polycrystalline particles of 12–23 nm in size. Further, the SAED concentric pattern of light scattering with well-defined diffraction spots was consistent and matched with maghemite's crystal structure (γFe_2O_3). The FTIR spectrum revealed a peak at 1450 cm^{-1} indicating iron oxyhydroxide formation as an intermediate having γ-FeOOH stretching bond vibrations. Conclusively, this study opens the possibility of the haloarchaea isolated from solar salterns for its exploitation in nanobiotechnology.

ARTICLE HISTORY
Received 25 October 2019
Accepted 6 July 2021

KEYWORDS
Archaea; ferric reductase; *Haloferax* sp. GUSF-1; maghemite

Introduction

Hypersaline environments such as solar saltern, salt lakes, and marshes located alongside estuaries serve as a water route for ferromanganese ore transportation in iron ore mining countries, including India and other coastal countries (Dessai and Nayak 2009; Miller et al. 2018). In hypersaline sediments, Fe can constitute up to 20% of the sediment by weight (Ussher et al. 2004). Fe^{3+} represents the dominant form of Fe in most salt lake environments (Mortimer et al. 2011). Long et al. (1992) have identified jarosite, goethite, and hydrous Fe oxides in hypersaline sediments, considering only abiotic aspects of Fe geochemistry and pertinent the role of microbes in Fe mineral transformation. There are only a few isolates from the hypersaline environment reported, reducing soluble Fe^{3+} (Pollock et al. 2007; Blum et al. 2009). Members of the family *Halobacteriaceae* growing in anaerobic - hypersaline conditions are reported to reduce Fe^{3+} to akaganeite [β-FeO(OH)] (Emmerich et al. 2012), suggesting the presence of an active microbial iron cycle at a salt concentration close to the solubility limit of NaCl. Likewise, McBeth et al. (2011) have studied micro-aerophilic Fe^{2+} oxidizing strain associated with the *Zetaproteobacteria* isolated from a microbial mat in the Great Salt Bay where salinity is between 0 and 2.5%.

Interaction of microorganisms with metal ions (Gadd and Raven 2010) often results in the formation of nanosized minerals of essential biotechnological significance (Gadd 2010). *Actinobacter* sp. is reported to form maghemite crystals during its aerobic invitro growth in ferric chloride and ferrous sulfide (Bharde et al. 2005; Bharde et al. 2008). Sundaram et al. 2012 have reported the extracellular synthesis of iron oxide Fe_3O_4 nanoparticles by *Bacillus subtilis* isolated from rhizosphere soil aerobically under dark conditions. Archaea such as *Thermoanaerobacter ethanolicus* and *Pyrobaculum islandicum* are also reported to form iron oxides in anaerobic environments having temperatures between 60 and 100 °C (Roh et al. 2002; Kashefi et al. 2008).

We previously isolated *Haloferax* sp.GUSF-1 (GenBank accession no.GU-1 KF796625), a haloarchaeon from a salt-pan of Goa-India, where the estuarine environment is known for being the receptacle and sink of metal ions such as iron and manganese due to ferromanganese mining activities (Alagarsamy 2006; Dessai and Nayak 2009). *Haloferax* sp. GUSF-1 is tolerant to various metal ions and metalloid with high minimum inhibitory concentrations of 200 mM

CONTACT Irene J. Furtado ijfurtado@unigoa.ac.in Department of Microbiology, Goa University, Taleigao Plateau, Goa, India

for Li^{2+}, 60 mM for As^{5+}, 3 mM for As^{3+}, 50 mM for Mn^{2+} 5 mM for Ni^{2+}, 2.5 mM for Cu^{2+} and Fe^{2+}/Fe^{3+} and 0.02 mM for Zn^{2+}/Cd^{2+}/and Hg^{2+}, respectively (Khandavilli et al. 1999; Braganca and Furtado 2001) and 1.5 mM for Pb^{2+}, 3 mM for Fe^{2+} and 0.02 mM for Zn^{2+} and Ag^{+} (Furtado and Naik 2009; Patil et al. 2014). Additionally, the culture is also reported to biosynthesize Ag^{o} and Te^{o} nanoparticles (Patil et al. 2014; Alvares and Furtado 2021) and rhodochrosite (Naik-Samant and Furtado 2019). It also tolerated hydrocarbon (Raghavan and Furtado 2000). Moreover, the ease of recovery of minerals synthesized by haloarchaeal culture makes it an ideal candidate for possible nanobiotechnological applications over other microbes and harsh chemical methods used for metal recovery (Giani et al. 2019).

In this study, we successfully studied the potential of the haloarchaeon *Haloferax* sp.GUSF-1 (GenBank accession no.GU-1KF796625) to form iron oxide mineral/s. We now communicate and record the formation of maghemite (γFe_2O_3) from Fe^{3+} during the haloarchaeon's growth under oxygen restricted -microaerophilic and low A_w conditions.

Materials and methods

Growth of Haloferax sp. GUSF-1 in the presence of Fe^{3+} under microaerophilic conditions

Haloferax sp. GUSF-1 was grown microaerophilically in a sterile glass vial filled to three third capacity with NSM medium (Raghavan and Furtado 2005) pH 6.0, which consisted of 0.2% sodium acetate instead of glucose as a sole source of carbon and 2 mM of $FeCl_3{\cdot}6H_2O$ as the source of Fe^{3+}. All the media components and chemicals used were of analytical grade and were dissolved into deionized high purity water (18 M^{-} cm) prepared by bubbling oxygen-free N_2 (99.99%) for 24 h. Vials of 25 ml capacity were filled to overflow with sterile medium, purged with N_2, aseptically. For five days, culture pregrown in NASM was inoculated into vials and incubated statically to ensure a microaerophilic environment in the vial. A control vial containing NASM with Fe^{3+} and without culture was also maintained likewise. Growth was monitored daily. Aliquots of culture broth were withdrawn with 2 mL N_2 purged sterile syringe and checked for absorbance A_{600} nm using UV–Vis spectrophotometer (UV2401 Shimadzu- Japan). All the glassware used was soaked overnight in 10% nitric acid (HNO_3), rinsed twice with MilliQ water, and oven-dried. All separations and analytical procedures were carried out under sterile nitrogen to ensure minimum oxygen.

Monitoring of reduction of Fe^{3+} during growth

For detection of Fe in the culture broth, aliquots were withdrawn aseptically with N_2 purged sterile syringe were centrifuged at 12,000 rpm for 10 min at 4 °C. The cell-free supernatant was transferred under N_2. To release metal inside the cells, the cell pellet was exposed to deoxygenated water for 30 min under sterile N_2, and the contents were centrifuged again at 12,000 rpm for 10 min at 4 °C and monitored for Fe^{2} by 1, 10- phenanthroline method of Mendham et al. (2009). The phenanthroline method was slightly modified by adding 1,10- phenanthroline reagent first to the test sample solution (1:1 *v/v*) and measuring the peak maxima at 510 nm for Fe^{2+} content. The Fe^{3+} content was analyzed by adding hydroxylamine (1:1 *v/v*), followed by 1,10- phenanthroline reagent (1:1). Samples from vail with Fe^{3+} and without culture, treated likewise, were used as controls. Total iron was also quantified by atomic absorption spectrophotometer (AAS).

Quantification of iron by atomic absorption spectrophotometer

The iron in the cell pellet and the supernatant was quantified aseptically by withdrawing 1 ml aliquot of the culture broth, followed by removing oxides with 200 µM ascorbate centrifuging at 10,000 rpm for 10 min. The cell pellet and the supernatant were separately digested using nitric acid (HNO_3) and sulfuric acid (H_2SO_4) (2:1 *v/v*). The clear digest was estimated for iron by atomic absorption spectrophotometer (AA-6300, Shimadzu). The standard of the iron solution of known concentration for AAS was prepared in 0.1 N HNO_3, in the range of 0–10 ppm to obtain a standard graph.

Estimation of iron reductase assay

Iron reductase activity was measured by the modified method of Dailey (Huyer and Page 1989). The assay was carried out in stoppered quartz cuvettes containing 200 µl of culture supernatant, 20 mM phosphate buffer, pH 7.2, 50 µl of NADH, 100 µl of ferrozine, 50 µl of 5 mM ferric citrate and incubated at room temperature for 20 min. The intensity of the purple color complex developed was measured at 562 nm by spectrophotometer (Shimadzu 2401 Japan) operating at a resolution of 1 nm. Control assay consisted of all of the reagents and culture supernatants of a culture grown in the absence of iron salt. Iron reductase thus detected, and present in the culture supernatant was confirmed by carrying out the assay in the presence of 100 µM of Zn^{2+} ions, an inhibitor of iron reductase (Crow et al. 2009).

Recovery of biomineral

The culture broth was centrifuged at 10,000 rpm for 15 min. The brown crystalline material recovered was resuspended in deionized deoxygenated water thrice to wash out culture broth impurities haloarchaeal cells. The brown material was then dried in glass petri-dish, at 80 °C till constant weight.

X-ray diffraction analysis

The recovered dried material was pulverized to a fine powder in an agate mortar and pestle and placed in the indentation of the X-ray slide, and sample material prepared flat with another glass slide. The slide containing the sample was placed in the sample holder of the X-ray machine and

scanned from 10 to 70°, at 0.02° 2θ intervals in a span of 40 s in a Rigaku Miniflex powder diffract meter equipped with an Ultima IV solid-state detector at a voltage of 40 kV and current of 20 mA with Cu-Kα radiation, $\lambda = 1.5418$ Å. The obtained XRD data was plotted, and FWHM was calculated using Origin 8.0 software. The crystal size was calculated by applying the Scherer's formula $D = k\lambda/\beta\cos\theta$ where D is the mean grain size, k is a constant, λ is the X-ray wavelength for Cu-Kα radiation, β is the FWHM of the diffraction peak in radians, and θ is the diffraction angle.

Scanning electron microscopy and electron diffraction X-ray analysis

To determine the mineral's chemical composition, the finely powdered material was coated as a thin layer on to the copper stubs and then sputter-coated with gold in a high vacuum evaporator. The stage was such that the stub was approximately 50 mm from the bottom of the sputter head. After sputtering the specimen with a 10–15 nm film of gold, the stub was placed in the scanning electron's sample chamber equipped with EDX (JEOL JSM-5800LV) and observed.

Transmission electron microscopy and selected area electron diffraction

A brown homogenous solution was prepared obtained by sonicating the mineral powder in 200 µl of MilliQ water for 5–10 min, a drop of which was placed onto 2 mm carbon-coated copper grids of 200–300 mesh allowed to air dry and placed in the sample chamber of the TEM (Philips CM200 Supertwin STEM), equipped with SAED, operated with the voltage of 200 keV and imaged.

Fourier transform Infrared analysis

KBr pellet of finely ground powder of mineral (1:10, *w/w*) was exposed to IR in a Prestige-21 FTIR (Shimadzu) to determine the functional groups in the mineral.

Results

Growth and reduction of Fe^{3+} by Haloferax sp.GUSF-1 in mineral salts medium

As depicted in Figure 1, *Haloferax* sp.GUSF-1 grew with a lag of 2 d, a log phase of 5 d in mineral salts medium with sodium acetate as a sole source of carbon at a growth rate of 1.3×10^2 gen h^{-1} and doubling time 76.8 min gen^{-1}, reached a maximum absorbance of 1.25 at A_{600}nm. The culture attained a stationary phase on the 8th d.

Further, in Fe^{3+} ($FeCl_3.6H_2O$) incorporated mineral salts medium, the culture grew with a shortened lag of only 1 d but an extended log phase of 2 d at a fold increase in the growth rate of 9.7×10^3 gen h^{-1} and a doubling time of 103 min gen^{-1}, attained a maximum absorbance of 1.5 which was followed by a stationary phase as during growth in acetate alone. On the fourth day, the concentration of $Fe^{2+}$and

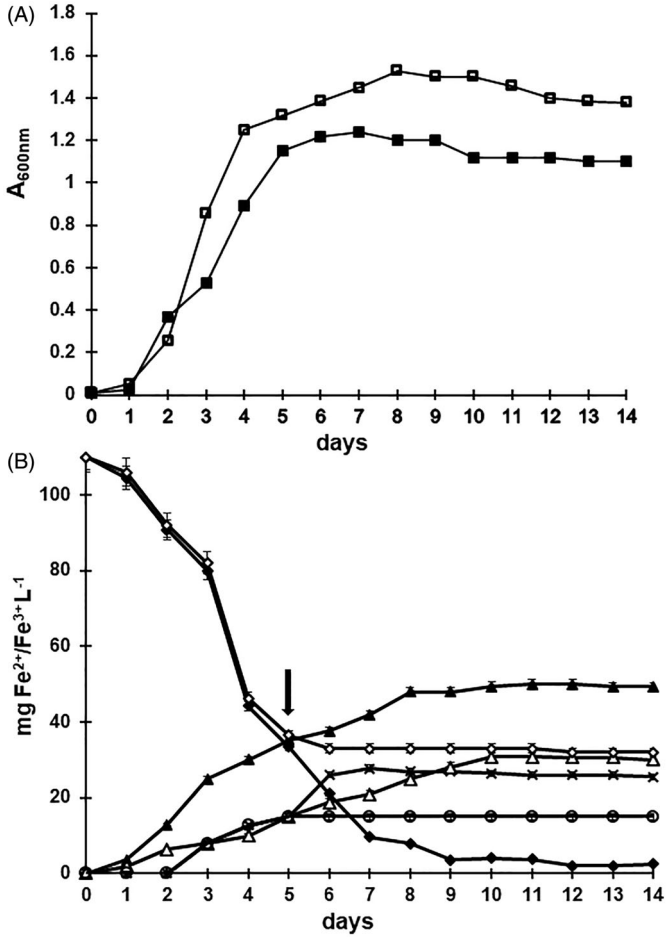

Figure 1. (A) *Haloferax* sp. GUSF-1 growing in: sodium acetate medium (NASM) (—●—), NASM containing Fe^{3+} ($FeCl_3.6H_2O$)(—□—). (B) Fe^{2+} inside the cells(—▲—),Fe^{2+} formed in the culture broth(—X—), Fe^{3+} remaining in culture broth(—♦—), Fe^{3+} inside the cells(—△—), Fe^{3+} in culture broth spiked with Zn^{2+} indicated with down arrow (↓) (—◇—) and Fe^{2+} formation arrested by Zn^{2+} ions(—O—). Error bar indicates standard error.

Fe^{3+} inside the cells increased to 30 mg L^{-1} and 10 mg L^{-1}, respectively, and to 50 mg L^{-1} of Fe^{2+} and 30.6 mg L^{-1} of Fe^{3+} by the ninth day, respectively, with a concomitant decrease in added Fe^{3+} to 3.6 mg L^{-1}. Interestingly, the accumulation of iron as Fe^{3+} and Fe^{2+} inside the cells is also accompanied by deposition of a brown colored amorphous substance and formation of Fe^{2+} in the culture broth, detectable to a concentration of 27 mg L^{-1} by the ninth day.

Iron reductase assay

The Fe^{3+} reductase activity was demonstrated in culture supernatant as a strong purple-colored ferrozine – ferrous iron complex with absorbance maxima at A_{562} nm (Figure 2). Ferric reductase activity was induced only in the presence of Fe^{3+}. Culture growing with Fe^{3+} when spiked with Zn^{2+} ions failed to show the ferric reductase activity and the accumulation of the brown material.

XRD

As seen in Figure 3, the X-ray diffractogram of the brown material d spacings of *hkl* planes at 2.96 (220), 2.514 (311),

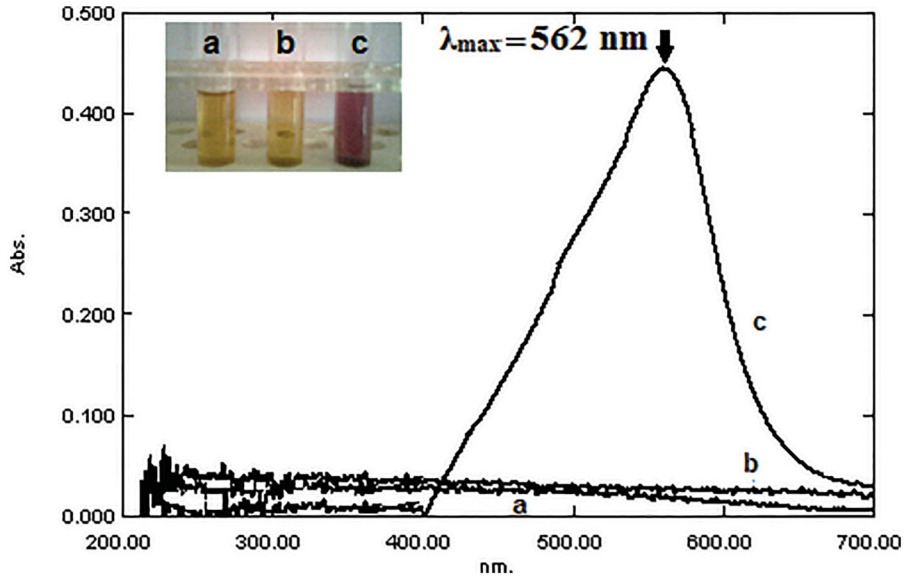

Figure 2. Spectral scan of: (a) supernatant of a culture grown in the absence of Fe^{3+}ions with negative ferric reductase activity, (b) supernatant of a culture grown in the presence of Fe^{3+} ions spiked with Zn^{2+} showing negative ferric reductase activity, (c) supernatant of a culture grown in the presence of Fe^{3+}exhibiting positive ferric reductase activity and inset showing the respective culture supernatants labeled as a, b, c.

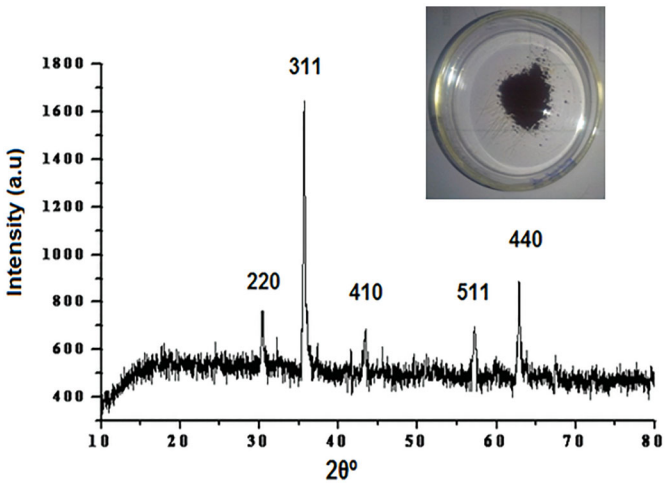

Figure 3. X-ray diffractogram of purified and powdered biomineral (inset) produced by *Haloferax* sp. GUSF-1 in NASM containing Fe^{3+} (JCPDS pattern 25-1402).

2.086 (410), 1.6 (511), 1.45 (440) matched with the Bragg's pattern and corroborated with records of JCPDS card no. 25-1402 characteristic for γFe_2O_3, i.e., maghemite. The application of Scherer's formula indicated an average size of the nano-crystallite formed in the biogenic reduction process to be of 23 nm mean size.

SEM-EDX analysis

The SEM profile of the mineral powder displayed cubic and irregularly shaped minute particles (Figure 4(a)). The EDX spectra showed peaks due to Fe at 0.6, 6.4, 6.6 keV. Peaks due to phosphorus, carbon, and oxygen were visible at 2.2, 1.6 and 0.2 keV, and 0.6 keV, respectively (Figure 4(b)).

TEM-SAED

The TEM micrographs revealed the clusters of electron-dense nanosized particles roughly in the range of 12-23 nm (Figure 5(a)). The concentric pattern of light scattering with well-defined diffraction spots in the SAED analysis (Figure 5(b)) was consistent with the maghemite crystal structure's polycrystalline nature and corroborated with the structural records for maghemite crystal in JCPDS chart no. 25-1402.

FTIR

In the FTIR spectrum, a broad absorption peak at 3400−3330 cm^{-1} corresponding to stretching and bending vibrations of water molecules was observed (Figure 6(a)). The rise at 1450 cm^{-1} was indicative of γ-FeOOH stretching bond vibrations assigned to iron oxyhydroxide possibly formed as an intermediate (Bharde et al. 2008). Two broad peaks, observed at 555 and 463 cm^{-1} in Figure 6(b), relate to Fe–O bond tetrahedral and octahedral stretching vibration mode, respectively, described by Kim et al. (2010) for γFe_2O_3.

Discussion

In this study, we have reported the potential of haloarchaeon *Haloferax* sp.GUSF-1to reduce Fe^{3+} to nanosized maghemite (γFe_2O_3) during its growth in acetate as a sole source of carbon at low Aw and microaerophilic conditions. A simultaneous increase in $Fe^{2+}$and Fe^{3+} inside the growing cells indicated the accumulation reduction of Fe^{3+} coupled to the oxidation of organic acetate as there are limited candidates for oxidation in the media. This result is similar to that of *Geobacter metallireducens* known as the first acetate oxidizing Fe^{3+} reducer (Lovley et al. 1993; Lovley 2004) that conserves energy and supports growth as is evident from the additional increase in absorbance in the presence of Fe^{3+} than the culture broth without Fe^{3+}. *Shewanella putrefaciens* is another bacteria that conserve energy to support growth by coupling the oxidation of lactate to reduce

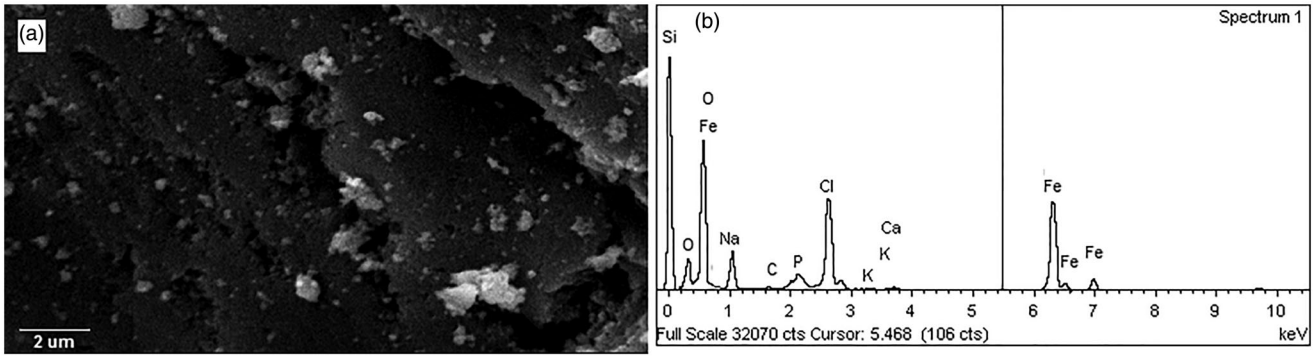

Figure 4. (a) Scanning electron micrograph and (b) energy dispersive X-ray profile of purified biomineral produced by *Haloferax* sp. GUSF-1.

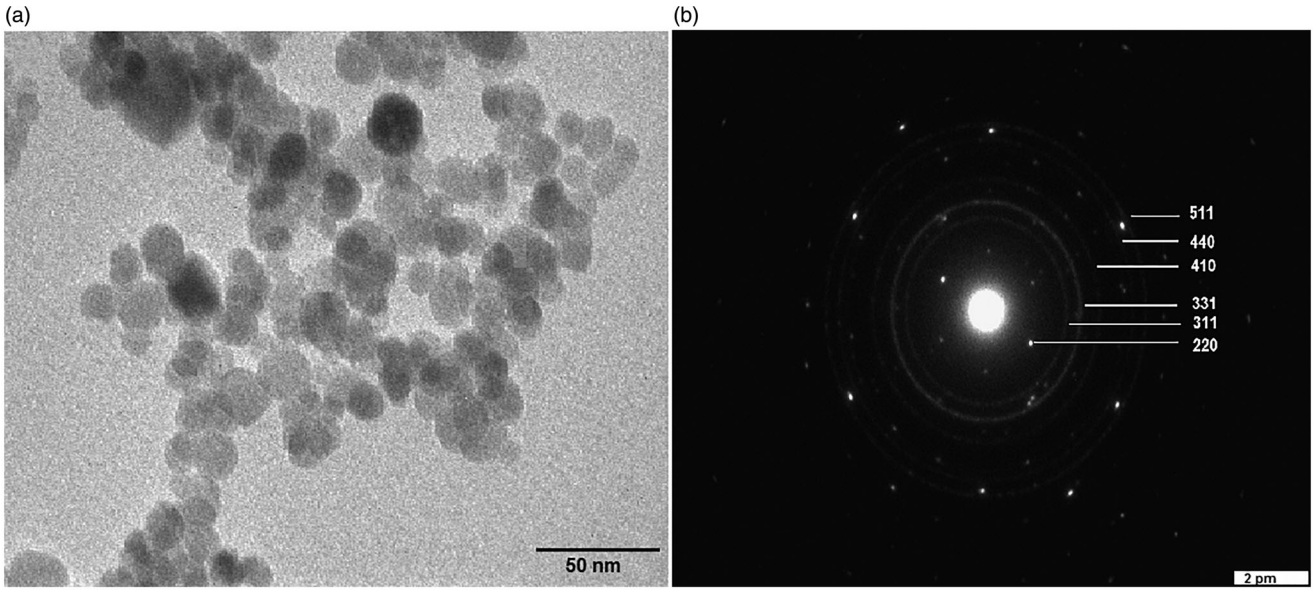

Figure 5. (a) TEM micrograph with (b) SAED of nanosized γFe_2O_3.

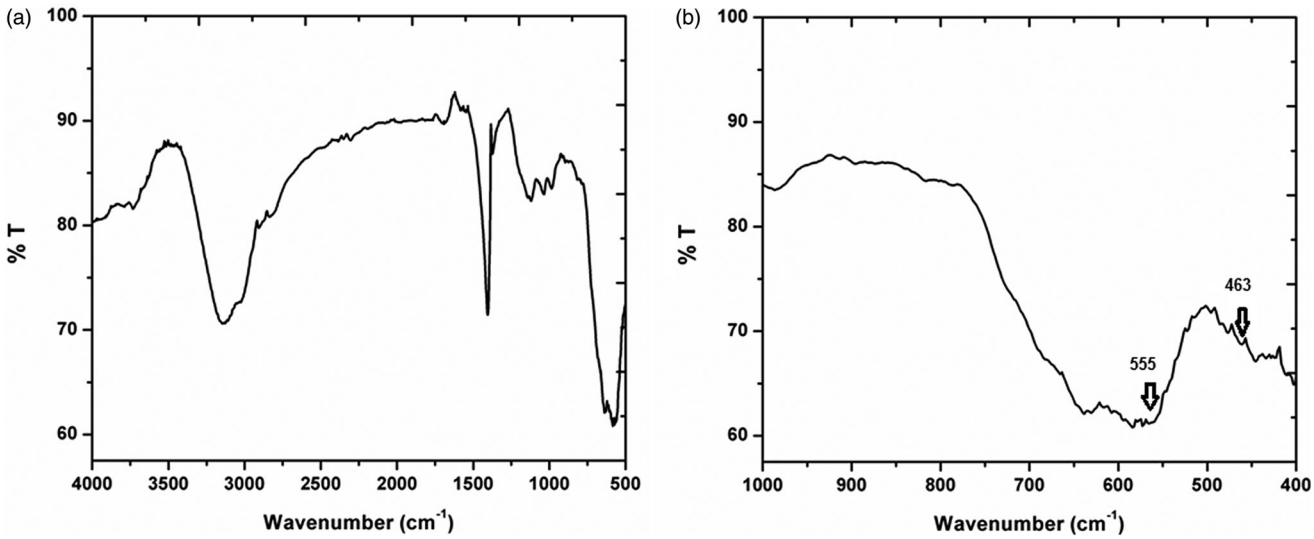

Figure 6. (a) FTIR spectrum of $\gamma Fe_2O_3$and (b) FTIR spectrum of γFe_2O_3 showing Fe–O stretching and bending vibrations.

Fe^{3+} (Lovley et al. 2004). The increase in cell density during growth in NASM with Fe^{3+} is expected to enhance and increase the microaerophilic conditions in the culture broth and preferentially contribute to the reduction of Fe^{3+} to a brown material. This is also supported by the fact that strict anaerobic conditions are not always required for metal reducing heterotrophs. However, metal reduction may be most rapid under microaerophilic conditions (Bazylinski and Frankel 2000). The accumulation of iron as Fe^{3+} and Fe^{2+} inside the cells accompanied by deposition of a brown

colored amorphous substance and formation of Fe^{2+} in the culture broth indicated the role of ferric reductase substantiated by the development of purple-colored ferrozine – ferrous iron complex in the culture supernatant of *Haloferax* sp.GUSF-1 was grown with Fe^{3+}, while no color complex was formed when grown without Fe^{3+}. Spiking the growth medium with Zn^{2+} ions, an inhibitor of ferric reductase (Crow et al. 2009), confirmed the role of reductase in reducing Fe^{3+} and formation of brown material in the culture broth. X-ray diffractogram revealed the brown material to be γFe_2O_3 chemically known as maghemite. To our understanding, *Haloferax* sp. GUSF-1 reduced Fe^{3+} to Fe^{2+} and then to γFe_2O_3, which was nano-size as calculated by Scherer's formula. The evidence of crystalline nature and presence of Fe–O peaks seen in SEM-EDX images was confirmed by Fe–O bond vibrations in the FTIR profile, which also showed a low-intensity oxyhydroxide peak at 1450 cm^{-1} acting as an intermediate. This result corroborated with that reported by Bharde et al. (2008), who stated the role of oxyhydroxide as an intermediate in the formation of maghemite by *Actinobacter* sp.

Further, TEM analysis confirmed the nano size of the material accompanied by SAED, showing well-defined diffraction spots consistent with the polycrystalline nature of biosynthesized maghemite crystal structure. Maghemite is exploited for magnetic recording, magnetic storage devices, ferrofluids, and contrast enhancers in MRI and other biomedical applications (Matsunaga et al. 2004; Silva et al. 2013). Moreover, the production of nanosized iron oxides, including maghemite, involves chemical and energy-intensive methods such as sol-gel, forced hydrolysis, sonochemical, and electrochemical, which impede biomedical applications of resulting material (Wu et al. 2015; Ali et al. 2016).

The use of a haloarchaeal candidate for the synthesis of mineral such as maghemite is advantageous over eubacterial candidates as they can withstand high salt (3–4 M NaCl) and varied temperature conditions (Amoozegar et al. 2017). All the more, haloarchaeal cells' property to lyse easily at low salt concentrations makes the recovery of minerals more cost-effective and less time-consuming without the use of harsh chemicals, making it an ideal candidate for nanobiotechnological applications (Giani et al. 2019).

We now conclusively infer that the haloarchaeon *Haloferax* sp.GUSF-1 is significant in the cycling of iron in the presence of acetate under saline culture conditions that have low water activity and are microaerophilic. We speculate that the biogenic process of the formation of maghemite by haloarchaeon *Haloferax* sp.GUSF-1 has exploitability for green synthesis of nanosized γFe_2O_3 and subsequently discern the potential applications that could be impacted by this microbe.

Acknowledgments

The authors are indebted to Dr. M. Shyamprasad and Mr.V. Khedekar, National Institute of Oceanography, Goa, India, for extending the SEM-EDX facility and Mr. G Prabhu for XRD profiling. We also thank the Indian Institute of Technology, Bombay, on for the TEM facility.

Disclosure statement

No potential conflict of interest was reported by the author(s).

References

Alagarsamy R. 2006. Distribution and seasonal variation of trace metals in surface sediments of the Mandovi estuary, west coast of India. Estuar Coast Shelf S 67(1–2):333–339.

Ali A, Zafar H, Zia M, Haq I, Phull AR, Ali JS, Hussain A. 2016. Synthesis, characterization, applications, and challenges of iron oxide nanoparticles. Nanotechnol Sci Appl 9:49–67.

Alvares JJ, Furtado IJ. 2021. Anti-Pseudomonas aeruginosa biofilm activity of tellurium nanorods biosynthesized by cell lysate of Haloferax alexandrinus GUSF-1(KF796625). Biometals. doi: 10.1007/s10534-021-00323-y

Amoozegar MA, Siroosi M, Atashgahi S, Smidt H, Ventosa A. 2017. Systematics of haloarchaea and biotechnological potential of their hydrolytic enzymes. Microbiology 163(5):623–645.

Bazylinski DA, Frankel RB. 2000. Biologically controlled mineralization of magnetic iron minerals by magnetotactic bacteria. In: Lovley DR, editor. Environmental microbe-mineral interactions. Washington DC:ASM Press p109–144.

Bharde AA, Parikh RY, Baidakova M, Jouen S, Hannoyer B, Enoki T, Prasad BLV, Shouche YS, Ogale S, Sastry M. 2008. Bacteria-mediated precursor-dependent biosynthesis of superparamagnetic iron oxide and iron sulfide nanoparticles. Langmuir. 24(11):5787–5794.

Bharde AA, Wani A, Shouche Y, Joy PA, Prasad BLV, Sastry M. 2005. Bacterial aerobic synthesis of nanocrystalline magnetite. J Am Chem Soc. 127(26):9326–9327.

Blum JS, Han S, Lanoil B, Saltikov C, Witte B, Tabita FR, Langley S, Beveridge TJ, Jahnke L, Oremland RS. 2009. Ecophysiology of "*Halarsenatibacter silvermanii*" strain SLAS-1T, gen. nov., sp. nov., a facultative chemoautotrophic arsenate respirer from salt-saturated Searles Lake, California. Appl Environ Microbiol 75(7):1950–1960.

Braganca J, Furtado I. 2001. Removal of cadmium from saline water using haloarcheal cell bioprocesses. Proceedings of 1st European Bioremediation Conference, Greece.

Crow A, Lawson TL, Lewin A, Moore GR, Le Brun NE. 2009. Structural basis for iron mineralization by bacterioferritin. J Am Chem Soc. 131(19):6808–6813.

Dessai DVG, Nayak GN. 2009. Distribution and speciation of selected metals in surface sediments, from the tropical Zuari estuary, central west coast of India. Environ Monit Assess. 158(1–4):117–137.

Emmerich M, Bhansali A, Behrens LT, Schroder C, Kappler A, Behrens S. 2012. Abundance, distribution, and activity of Fe(II)-oxidizing and Fe(III)-reducing microorganisms in hypersaline sediments of Lake Kasin, southern Russia. Appl Environ Microbiol. 78(12):4386–4399.

Furtado I, Naik S. 2009. SABIC 2009. Proceedings of International Symposium on Advanced Inorganic Biological Chemistry; Nov 4–7; Tata Institute of Fundamental Research Centre, Mumbai, India. p113–114.

Gadd GM, Raven JA. 2010. Metals, minerals and microbes: geomicrobiology and bioremediation. Geomicrobiol J 27(6–7):491–519.

Gadd GM. 2010. Metals, minerals and microbes: geomicrobiology and bioremediation. Microbiology. 156(Pt 3):609–643.

Giani M, Garbayo I, Vilchez C, Espinosa RMM. 2019. Haloarchaeal carotenoids: healthy novel compounds from extreme environments. Mar Drugs 17(9):524.

Huyer M, Page WJ. 1989. Ferric reductase activity in *Azotobacter vinelandii* and its inhibition by Zn2+$^{+}$. J Bacteriol 171(7):4031–4037.

Kashefi K, Moskowitz BM, Lovley DR. 2008. Characterization of extracellular minerals produced during dissimilatory Fe(III) and U(VI) reduction at 100 degrees C by *Pyrobaculum islandicum*. Geobiology 6(2):147–154.

Khandavilli S, Sequeira F, Furtado I. 1999. Metal tolerance of extremely halophilic bacteria isolated from estuaries of Goa, India. Ecol Environ Conserv 5:149–152.

Kim T, Nunnery GA, Jacob K, Schwartz J, Liu X, Tannenbaum R. 2010. Synthesis, characterization, and alignment of magnetic carbon nanotubes tethered with maghemite nanoparticles. J Phys Chem C 114(15):6944–6951.

Long DT, Fegan NE, McKee JD, Lyons WB, Hines ME, Macumber PG. 1992. Formation of alunite, jarosite and hydrous iron-oxides in a hypersaline system—Lake Tyrrell, Victoria, Australia. Chem Geol 96(1–2):183–202.

Lovley DR, Giovannoni SJ, White DC, Champine JE, Phillips EJ, Gorby YA, Goodwin S. 1993. *Geobacter metallireducens* gen. nov. sp. nov., a microorganism capable of coupling the complete oxidation of organic compounds to the reduction of iron and other metals. Arch Microbiol 159(4):336–344.

Lovley DR, Holmes DE, Nevin KP. 2004. Dissimilatory Fe(III) and Mn(IV) reduction. Adv Microb Physiol 49:219–286.

Matsunaga T, Okamura Y, Tanaka T. 2004. Biotechnological application of nano-scale engineered bacterial magnetic particles. J Mater Chem 14(14):2099–2105.

McBeth JM, Little BJ, Ray RI, Farrar KM, Emerson D. 2011. Neutrophilic iron-oxidizing "*Zetaproteobacteria*" and mild steel corrosion in nearshore marine environments. Appl Environ Microbiol 77(4):1405–1412.

Mendham J, Denney RC, Barnes JD, Thomas M, Sivasankar B. 2009. Vogel's Textbook of Quantitative Chemical Analysis. India: Pearson Education, p114–115.

Miller KA, Thompson KF, Johnston P, Santillo D. 2018. An overview of seabed mining including the current state of development, environmental impacts, and knowledge gaps. Front Mar Sci 4:418.

Mortimer RJ, Galsworthy AM, Bottrell SH, Wilmot LE, Newton RJ. 2011. Experimental evidence for rapid biotic and abiotic reduction of Fe (III) at low temperatures in salt marsh sediments: a possible mechanism for formation of modern sedimentary siderite concretions. Sedimentology 58(6):1514–1529.

Naik-Samant S, Furtado I. 2019. Formation of rhodochrosite by *Haloferax alexandrinus* GUSF-1. J Clust Sci 30(6):1435–1441.

Patil S, Fernandes J, Tangasali R, Furtado I. 2014. Exploitation of *Haloferax alexandrinus* for biogenic synthesis of silver nanoparticles antagonistic to human and lower mammalian pathogens. J Clust Sci 25(2):423–433.

Pollock J, Weber KA, Lack J, Achenbach LA, Mormile MR, Coates JD. 2007. Alkaline iron(III) reduction by a novel alkaliphilic, halotolerant, *Bacillus* sp. isolated from salt flat sediments of Soap Lake. Appl Microbiol Biotechnol 77(4):927–934.

Raghavan TM, Furtado I. 2000. Tolerance of an estuarine halophilic archaebacterium to crude oil and constituent hydrocarbons. Bull Environ Contam Toxicol 65(6):725–731.

Raghavan TM, Furtado I. 2005. Expression of carotenoid pigments of haloarchaeal cultures exposed to aniline. Environ Toxicol 20(2): 165–169.

Roh Y, Liu SV, Li G, Huang H, Phelps TJ, Zhou J. 2002. Isolation and characterization of metal-reducing *Thermoanaerobacter* strains from deep subsurface environments of the Piceance Basin, Colorado. Appl Environ Microbiol 68(12):6013–6103.

Silva MF, Winkler HAA, de Oliveira DM, Agüeros M, Peñalva R, Irache JM, Pineda EA. 2013. Optimization of maghemite-loaded PLGA nanospheres for biomedical applications. Eur J Pharm Sci 49(3):343–351.

Sundaram PA, Augustine R, Kannan M. 2012. Extracellular biosynthesis of iron oxide nanoparticles by *Bacillus subtilis* strains isolated from rhizosphere soil. Biotechnol Bioproc E 17 (4):835–840.

Ussher SJ, Achterberg EP, Worsfold PJ. 2004. Marine biogeochemistry of iron. Environ Chem 1(2):67–80.

Wu W, Wu Z, Yu T, Jiang C, Kim WS. 2015. Recent progress on magnetic iron oxide nanoparticles: synthesis, surface functional strategies and biomedical applications. Sci Technol Adv Mater 16(2):023501.